Structural Configuration and Thermal Analyses of Composite Films of Poly (Methyl methacrylate)/Lead Oxide Nanoparticles

Sarah A. Elawam[1], Hoda M. Abou-Shady[2], Wafaa M. Morsi[3], Osiris W. Guirguis[1]
[1]*Biophysics Department, Faculty of Science, Cairo University, Giza, Egypt*
[2]*Physics Department, Faculty of Science, Cairo University, Giza, Egypt*
[3]*Building Physics Institute, Housing and Building National Research Center (HBRC), Giza, Egypt*

Abstract

In the present work, solution-cast method was used to prepare thin films of poly(methyl methacrylate)/lead oxide nanoparticles composites [PMMA/PbO(NPs)] due to their importance in different applications. X-ray diffraction analyses, scanning electron microscope (SEM), Fourier transform infrared spectroscopy (FTIR) and thermal properties were employed to characterize the structure properties of such composite. The XRD patterns suggested that the miscibility between the amorphous components of PMMA and PbO nanoparticles was possible. The SEM images show the distributions and dispersions of PbO nanoparticles on the surface of PMMA and the composite films. From the FTIR results, the performance properties of PMMA depend on the concentration of PbO nanoparticles. In addition, thermal results showed variations in the melting temperature (T_m), shape and area of thermal peaks which were attributed to the different degrees of crystallinity and the existence of interactions between PMMA and PbO nanoparticles molecules.

Keywords — *Biomaterials, poly(methyl methacrylate); lead oxide nanoparticles; polymer–nanoparticles composites; thermal analyses; structure configuration*

I. INTRODUCTION

Nano-materials were attracted the interesting of many researchers due to their physical and chemical properties as well as their applications in different fields [1]-[4]. Also, composite materials from polymers and nanoparticles (NPs) have advanced applications in the field of material science [5]-[7].

Poly(methyl methacrylate) (PMMA) is one of the best organic thermoplastic materials. PMMA is a nondegradable biopolymer, has thermal stability, easy shaping and weather resistance [8]. PMMA has wide applications in different medical fields. PMMA was used [9]-[13]: (1) in optical devices (e.g., optical lenses); as a means of securing prosthetic implants in skeletal antibiotic delivery system purposes for the treatment of osteomyelitis and osseous infections; support medium for the embedding of intact undecalcified bone; and for subsequent histological examination and calcified tissue sectioning.

Lead oxides can be formed in one of four numerous phases: PbO (α, β and amorphous), Pb_2O_3, Pb_3O_4, PbO_2 (α, β and amorphous). PbO has two polymorphic forms: (1) red α-PbO, (stable at low temperature), and (2) yellow β-PbO stable at temperatures higher than 425 ^oC) [14], [15]. Synthesized PbO nano-powders were produced and characterized by using several methods [15]-[17]. Nanocrystals of the two polymeric forms (α- and β-PbO) were obtained via the calculation of both lead citrate and lead oxalate [18].

Lead oxide nanoparticles [PbO(NPs)] were widely used in various applications in different fields such as; gamma ray protective clothing, X- and gamma rays shielding radiation, magnetic imagining, batteries, X-ray sensing application and drug delivery [19]-[23]. Due to the wide band gap and high refractive index of PbO(NPs), their rod and spherical shaped have antibacterial applications. Moreover, PbO nanoparticles were amphoteric react with both acid and base [24].

In the present work, five composite films of [PMMA/PbO(NPs)] were prepared using solution-cast method. Characterization of such composite film was employed by using X-ray diffraction analyses, scanning electron microscope (SEM), Fourier transform infrared spectroscopy (FTIR) as well as thermal properties [differential scanning calorimetry (DSC) and thermogravimetric analysis (TGA)] to reveal the relationship of the structure properties of PMMA to be used in different technological applications.

II. MATERIALS AND METHODS

A. Materials and Sample Preparation

Poly(methyl methacrylate) powder of chemical formula $[CH_2C(CH_3)(CO_2CH_3)-]_n$ with average molecular weight of 320,000 g/mol was

surgery; as a delivery agent for local high-dose antibiotics to treat soft tissue; for UK. Lead diacetate of chemical formula [$Pb(CH_3COO)_2$] with average molecular weight 279.33 g/mol and oxalic acid [$C_2H_2O_4$] of molecular weight 126.07 g/mol supplied from Adwik (Egypt) were used.

The sol–gel process was used to get lead monoxide nanoparticles [PbO(NPs)] [14], [25], [26]. A yellow-greenish powder of lead monoxide was obtained. The X-ray diffraction (XRD) pattern (data not shown) showed that the obtained PbO nano-powder was a mixture of orthorhombic β-PbO and tetragonal α-PbO phases with average crystalline size of about 84 nm.

Different ratios, X (= 0, 0.26, 0.48, 0.52, 0.78 and 1.00 wt%) of the prepared PbO(NPs) were added in to PMMA as [14]:

$$X = 100\ [W_{NPs}/(W_{NPs} + W_{P})]$$

Where W_{NPs} is the weight of PbO(NPs) and W_P is the weight of pure PMMA. Composite films of PMMA/PbO(NPs) [100.00/0.00, 99.74/0.26, 99.48/0.52, 99.22/0.78 and 99.00/1.00 wt/wt%] were prepared by casting method [14], [25-27]. PbO(NPs) were added to complete solution of PMMA in the appropriate ratio under vigorous stirring at 60 °C to prevent agglomeration. The solution were cast into stainless steel Petri dishes and placed in an oven at 60 °C for 24 h in air to obtain films of uniform thickness of about 0.01 mm.

Characterizations of the Prepared CompositeFilms

The X-ray diffraction (XRD) measurement of the prepared PMMA/PbO(NPs) composite films was recorded by using Phillips PW1840 X-Ray Diffractometer (USA) with an anode tube of CuK_α radiation (λ = 1.54056 Å), operated at 40 kV and 25 mA.

The surfaces of the prepared PMMA/PbO(NPs) composite films were investigated using scanning electron microscope (SEM; Inspect S, FEI, Holland) operated at 15 kV and with magnification X400. The samples were sputtered with gold by a sputter coater as an adhesive and electronic conductor.

The Fourier transform infrared absorption (FTIR) spectra of the prepared composite films under investigations were performed over the range 4000-500 cm^{-1} using a Bruker Vector 22 Spectrophotometer (Germany) with a resolution of 4 cm^{-1} and accuracy better than ±1%.

The thermal analyses of the prepared PMMA/PbO(NPs) composite films were studied by using Differential Scanning Calorimetry (DSC) supplied from Alfa Aesar, GmbH & Co.,

Figure 1 shows the X-ray diffraction patterns of the prepared PMMA/PbO(NPs) composite films. It is noticed from the figure that the patterns of the prepared composites exhibit weak diffraction lines superimposed on two broad humps. The first hump extends from $2\theta = 8^o$ to 26^o and the second one extends from $2\theta = 26^o$ to 37^o. The broadening of the peak indicates the amorphous nature and/or poor ordering of this composite and also does not depend on the concentration of PbO nanoparticles in the PMMA network. In addition, no identification crystalline species were present in any composite.

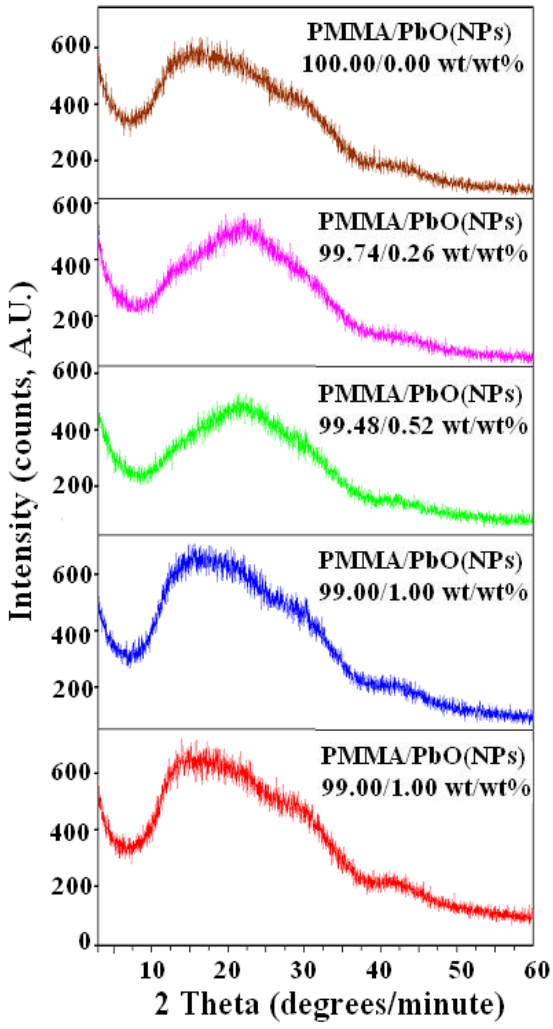

Fig. 1 XRD Patterns of PMMA/PbO(NPs) Composite Films

B. Scanning Electron Microscope

The distributions and dispersions of PbO nanoparticles were investigated on the surface of PMMA and the composite films by using scanning electron microscope (SEM). Figure 2 illustrates SEM images for pure PMMA (a) and some selected PMMA/PbO(NPs) composite films (b and c). It was noticed from the images that, numbers of

model Schimadzu DSC-50 (Kyoto, Japan) and Thermogravimetric Analyzer model Schimadzu TGA-50H (Kyoto, Japan). The DSC and TGA analyses cover the range from 25 to 650 ^{o}C were performed under nitrogen atmosphere of rate of flow 20 mL/minute and at rate of heating of 10^{o}C/minute. The average weight of the sample was about 6.53834 mg. The standard uncertainty of the sample weight measurement was ± 1%.

III. RESULTS AND DISCUSSION

A. X-Ray Diffraction (XRD)

obtained results showed that the addition of PbO nanoparticles with small amount to PMMA could be used to control the structural properties of PMMA polymer [28].

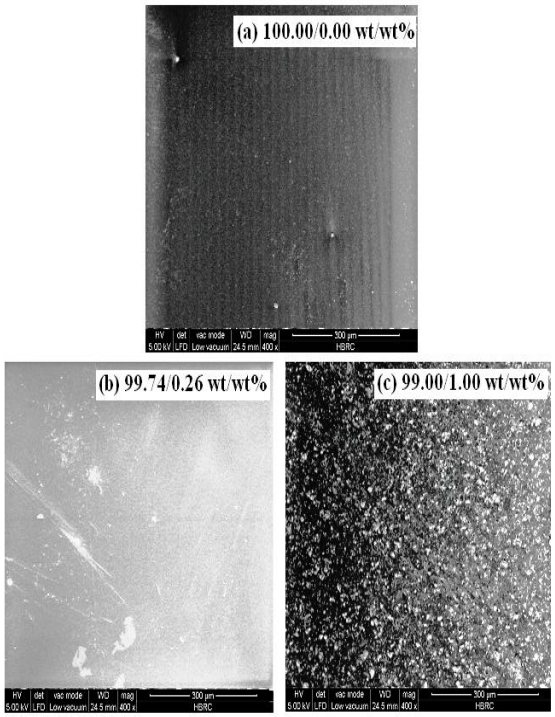

Fig. 2 SEM images for PMMA/PbO(NPs) composite films

C. Fourier Transform Infrared (FTIR) Spectral Analyses

The FTIR absorbance spectra of the prepared PMMA/PbO(NPs) composite films in the frequency range 4000-500 cm^{-1} were shown in Fig. 3. The chemical assignments of PMMA/PbO(NPs) composites were illustrated in Table 1. It was noticed that the present functional groups detected from the FTIR spectrum of PMMA were in agreement with that previously reported by several investigators [9], [29]-[34] and was comparable to that of its composites.

It was observed from the figure and the table that, the spectra of the prepared composites exhibit absorption that arises from C-H stretching of the methyl groups occurs in the region of 3000-2850 agglomerations were formed with increasing PbO nanoparticles content up to 1.00 wt% (image c) which indicate that good dispersion of PbO nanoparticles on the surface of the PMMA. These C-H bending. The bands at about1190, 1145 and 1065 cm^{-1} were attributed to C-O stretching vibration, asymmetric vibration of C-C group and C-H bending vibration, respectively. The band at about 989 cm^{-1} may be attributed to out-of-plane C=C–H bends. The band at about 966 cm^{-1} was attributed to CH wagging. The band at about 913 cm^{-1} corresponds to the =CH rocking mode. The bands at about 842 cm^{-1} was assigned to -CH_2 rocking vibration group. The band at about 750 cm^{-1} corresponds to out-of-plane C-H bending. The band at about 702 cm^{-1} corresponds to ring deformation vibration. Finally, the band in the region from 684-665 cm^{-1} corresponds to bending mode of the phenyl group ν (benzene ring). In addition, it was also illustrated from Fig. 3 that a clear deviation was observed in the absorbance bands of the PMMA/PbO(NPs) composites when compared with that detected for pure PMMA. The decrease and/or increase in the intensity indicate that there is a change in the molecular configuration of the PMMA network.

D. Differential Scanning Calorimetry (DSC)

Figure 4 and Table 2 illustrate the variation of DSC curves of the prepared PMMA/PbO(NPs) composite films to examine the effect of the presence of different contents of PbO nanoparticles. It is clear from the figure and the table that, endothermic and exothermic peaks were observed at about 365 and 502 ^{o}C, respectively, corresponding to the decomposition temperatures of the pure PMMA which is in agreement with previously studied in the literature [35]. For the composites PMMA/PbO(NPs), the decomposition endotherms in the range 360-365 ^{o}C were slightly broadened and the peak temperature value did not show remarkable shift with increasing the content of PbO nanoparticles. Other exothermic peaks were detected at about 429 & 506 ^{o}C for the composite 99.48/0.52 wt/wt%, and 422 & 498 ^{o}C for the composite 99.22/0.78 wt/wt%. For the composite 99.00/1.00 wt/wt%, new decomposition endotherm was detected at about 266 ^{o}C and the exothermic peak was disappeared.

In addition, the values of the heat of fusion detected from the area under the endothermic and exothermic peaks of decomposition steps and its rate has been found to be very effective to evaluate fire hazards. In addition, it was noticed from the figure and the table that, difference in shape and area of the decomposition endothermic and exothermic were observed. It can be shown that decrease in enthalpy of fusion and decrease in melting temperature values were detected. This indicate that change in the crystalline structure can results from PMMA

cm^{-1}, which contain four distinct peaks at about 2996, 2950, 2928, and 2874 cm^{-1} resulting from asymmetrical and symmetrical stretching modes of C-H bonding in the methyl group, respectively. The peak at about 1725 cm^{-1} represents C=O double bond stretching vibration of the aliphatic esters was used to characterize the existence of PMMA in the composite. The band at about 1485 cm^{-1} corresponds to the methylene C-H bends group. The band in the region of 1435-1450 cm^{-1} corresponds to the O-CH_3 deformation or stretching group. The bands at about 1386 cm^{-1} was associated with CH_2 deformation. The band at about1271 cm^{-1} is associated with C-O stretching vibration. The band at about 1240 cm^{-1} can be attributed to the in plane polymer and PbO nanoparticles interactions in the amorphous phase of PMMA and also disorder in the crystals was created causing the reduction in the enthalpy of the phase change [36], [37].The initial scission of PMMA may happened by random scission (C-C bonds) of the main chain and/or hemolytic scission of the methoxycarbonyl side groups (-$COOCH_3$). Random C-C scission was the dominant mechanism which decomposes PMMA into methyl methacrylate as a major product such as CO_2, CO, CH_3OH, CH_4 and char. PMMA ignites at 460 ^oC and burns forming CO_2, CO), H_2O and low molecular weight compounds, including formaldehyde [38], [39].

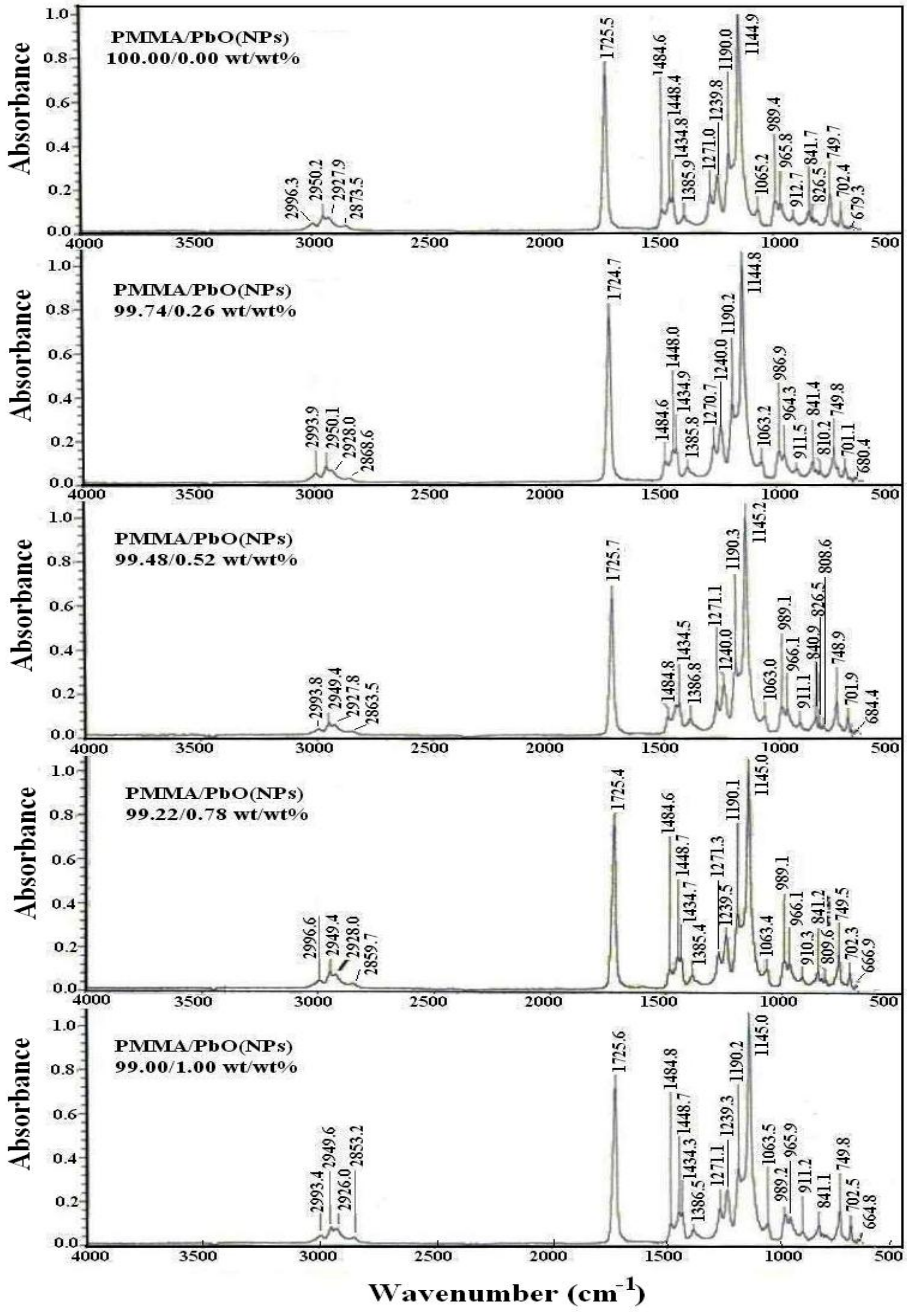

Fig. 3 FTIR spectra of PMMA/PbO(NPs) composite films

TABLE 1

POSITIONS AND ASSIGNMENTS OF BANDS OF PMMA/PbO(NPs) COMPOSITES

Wavenumber (cm^{-1}) PMMA/PbO(NPs) composites (wt/wt%)					Assignments
10.000/0.00	**99.74/0.26**	**99.48/0.52**	**99.74/0.78**	**99.00/1.00**	
2996.3	2993.9	2993.8	2996.6	2993.4	Asymmetrical stretching modes of C-H bonding in the methyl group
2950.2	2950.1	2949.4	2949.4	2949.6	Symmetrical stretching modes of C-H bonding in the methyl group
2927.9	2928.0	2927.8	2928.0	2926.0	Asymmetric CH_2 stretch
2873.5	2868.6	2863.5	2859.7	2853.2	Symmetric CH_2 stretch
1725.5	1724.7	1725.7	1725.4	1725.5	C=O double bond stretching vibration of the aliphatic esters
1484.6	1484.6	1484.8	1484.6	1484.8	Methylene C-H bends
1434.8	1434.9	1434.5	1434.7	1448.7	O-CH_3 deformation or stretching
1385.9	1385.8	1386.8	1385.4	1386.5	CH_2 deformation
1271.0	1270.7	1271.1	1271.3	1271.1	Associated with C-O stretching vibration
1239.8	1240.0	1240.0	1239.5	1239.3	In plane C-H bending
1189.0	1190.2	1190.3	1190.1	1190.2	C-O stretching
1144.9	1144.8	1145.2	1144.9	1145.0	Asymmetric stretching vibration of C-C group
1065.2	1063.2	1063.0	1063.4	1063.5	C-H bending vibration
989.4	986.9	989.0	989.1	989.2	Out of plane C=C–H bends
965.8	964.3	966.1	966.1	965.9	CH wagging
912.7	911.5	911.1	910.3	911.2	=CH rocking mode
841.7	841.4	840.9	841.2	841.1	CH_2 rocking vibration mode
749.7	749.8	749.5	749.5	749.8	Out of plane C-H bending
702.4	701.1	701.9	702.3	702.5	Ring deformation vibration
679.3	680.4	684.4	666.9	664.8	Bending mode of the phenyl group ν (benzene ring)

E. Thermal Gravimetric Analysis (TGA)

Thermal stability and thermal decomposition of polymers was understood by using thermal gravimetric analysis (TGA). Figure 5 shows the TGA curves of the prepared PMMA/PbO(NPs) composite films. The curves indicated four weight loss steps. Table 3 illustrates the % weight loss and the mid point temperature of these steps at the melting temperature region. From the figure for the pure PMMA curve, it is noticed that, three weight loss steps were shown. The first loss step starting above 120 ^oC with small values of % weight loss confirms the presence of a thermal process which may be attributed to splitting or volatilization of small molecules and/or PMMA monomers and explain the existence of physical transition [40]. The second loss step starting above 200 ^oC and may be attributed to melting and degradation of different morphological components forms the complex structure of PMMA. This second step corresponds to the weight loss caused by the decomposition of the PMMA structure [8]. In addition, it is characterized by the presence of the melting second step mid-point temperature of the PMMA/PbO(NPs) composites was smaller than that detected for the pure PMMA. A lowest decrease of about 9% for the composite 99.22/0.78 wt/wt% was detected.

For the third step, the endothermic decompositions of 99.74/0.26, 99.48/0.52 and 99.22/0.78 wt/wt% composites occur at about 369, 360 and 365 ^oC, respectively, and they were lower than that of the pure PMMA (about 376 ^oC). This may be attributed to that as the content of PbO nanoparticles increases in the PMMA polymer; the composites became more thermally stable which indicate better dispersed of PbO nanoparticles in PMMA matrix. For composite 99.00/1.00 wt/wt%, the decomposition mid-point temperature was about 348 ^oC which shows the highest % weight loss and greater than that of the pure PMMA sample (about 5%) and the lowest value was detected for composite 99.74/0.26 wt/wt% (about 3%).

Table 4 listed, the total % weight loss and residue % data at the end of the thermal degradation of the prepared PMMA/PbO(NPs) composites. It is noticed that, the total % weight loss did not show remarkable change by increasing the concentration of PbO nanoparticles. This means that the

endotherm peak at about 367 °C. It is noticed from Table 3 that, the values of the

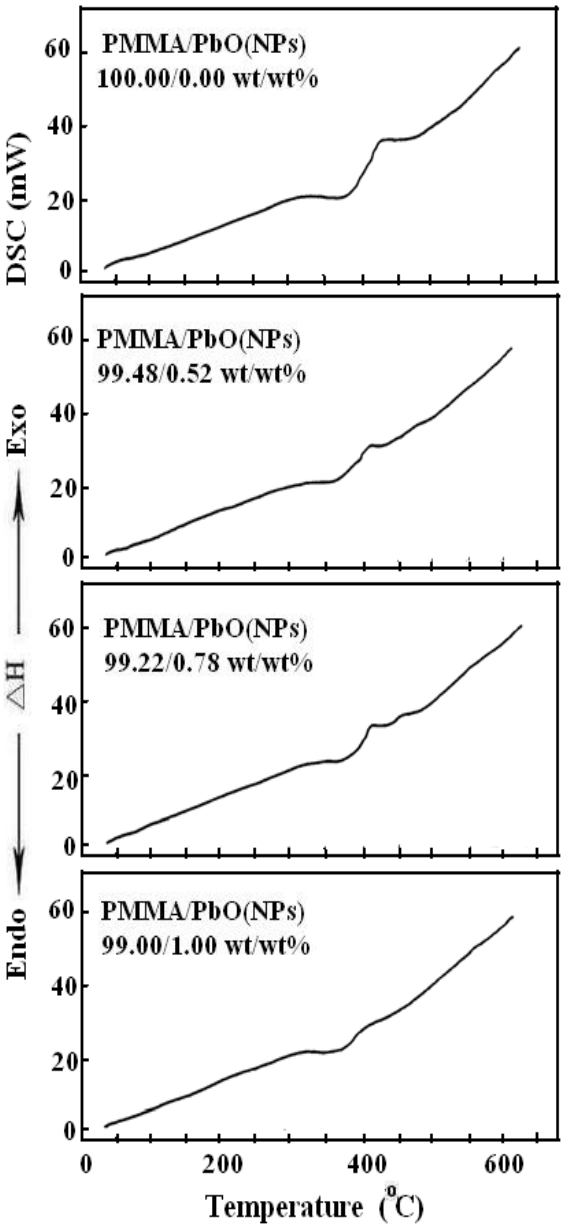

Fig. 4 DSC curves of PMMA/PbO(NPs) composite films

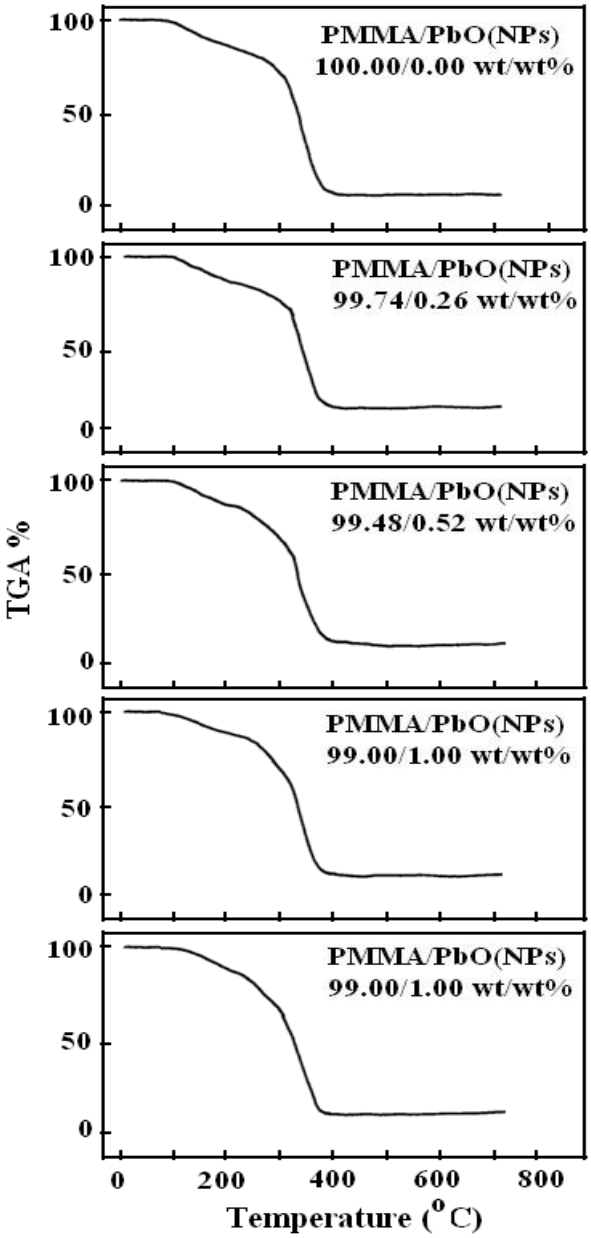

Fig. 5 TGA curves of PMMA/PbO(NPs) composite films

TABLE 2

VALUES OF TRANSITION TEMPERATURE (T_m) AND ASSOCIATED HEAT OF FUSION (ΔH) FOR PMMA/PbO(NPs) COMPOSITES

PMMA/PbO(NPs) composites (wt/wt%)	Melting transition region							
	First step		Second step		Third step		Fourth step	
	T_m (°C)	ΔH (J/g)	T_m (°C)	ΔH (J/g)	T_m (°C)	ΔH (J/g)	T_m (°C)	ΔH (J/g)
100.00/0.00	-	-	364.89	-148.61	-	-	501.74	221.22
99.48/0.52	-	-	360.13	-94.79	428.59	72.25	505.89	16.96
99.22/0.78	-	-	364.40	-76.42	421.72	50.42	496.78	22.18
99.00/1.00	265.80	-6.62	363.78	-109.30	-	-	-	-

TABLE 3

TGA DATA FOR PMMA/PbO(NPs) COMPOSITES

PMMA/PbO(NPs) composites (wt/wt%)	At melting transition region					
	First step		Second step		Third step	
	% weight loss	Mid point temperature (^{o}C)	% weight loss	Mid point temperature (^{o}C)	% weight loss	Mid point temperature (^{o}C)
100.00/0.00	10.711	163.27	5.684	225.94	80.322	367.10
99.74/0.26	12.640	158.31	7.546	209.50	77.880	368.58
99.48/0.52	9.299	156.83	4.617	207.86	81.745	360.02
99.22/0.78	7.373	152.64	5.998	206.50	83.043	365.40
99.00/1.00	8.968	163.36	5.310	215.71	83.987	348.49

table 4
total % weight loss and residue % data for pmma/pbo(nps) composites

PMMA/PbO(NPs) composites (wt/wt%)	Total % weight loss	Residue % *
100.00/0.00	96.717	3.283
99.74/0.26	98.066	1.934
99.48/0.52	95.661	4.339
99.22/0.78	96.414	3.586
99.00/1.00	98.265	1.735

* Residue % = 100 - Total % weight loss

prepared composites became more thermally stable and they were more resistant to fire hazards which indicate better dispersed of PbO nanoparticles in PMMA matrix.

IV. CONCLUSIONS

In the present work, the X-ray diffraction (XRD) analysis showed no identification crystalline species were present in the prepared PMMA/PbO(NPs) composites. The SEM images that illustrated numbers of agglomerations were formed with increasing PbO nanoparticles content up to 1 wt% which indicates that good dispersion of PbO nanoparticles on the surface of the PMMA.

From FTIR data, a clear deviation was observed in the absorbance bands of the PMMA/PbO(NPs) composites when compared with that detected for pure PMMA. In addition, the decrease and/or increase in the intensity indicate that there is a change in the molecular configuration of the PMMA network.

On other hand, from the obtained results of differential scanning calorimetry (DSC) and thermal gravimetric analysis (TGA), difference in shape and area of the decomposition endothermic and exothermic were observed. In addition, the total % weight loss did not show remarkable change by increasing the concentration of PbO nanoparticles up to 1 wt%. These variations mean that the prepared composites became more thermally stable and they were more resistant to fire hazards which indicate better dispersed of PbO nanoparticles in PMMA matrix. These results were in agreement with that of the obtained data in X-ray diffraction and SEM.

ACKNOWLEDGEMENTS

This work was carried out through the collaboration between Biophysics Department; Physics Department, Faculty of Science, Cairo University; and Building Physics Institute, Housing and Building National Research Center (HBRC), Giza, Egypt.

REFERENCES

[1] M. Salavati-Niasari, F. Mohandes, and F. Davar, "Preparation of PbO nanocrystals via decomposition of lead oxalate," *Polyhedron*, vol. 28, pp. 2263–2267, 2009.

[2] E. E. Ferg, T. Phangalala, and T. Dyl, "A new look at determining acid absorption of lead oxide used in the manufacturing of Pb-acid batteries," *J. Appl. Electrochem.*, vol. 40, pp. 383-391, 2010.

[3] S. Liu, Z. - R. Tang, Y. Sun, J. C. Colmenares, and Y. - J. Xu, "One-dimension-based spatially ordered architectures for solar energy conversion," *Chem. Soc. Rev.*, vol. 44, pp. 5053-5075, 2015.

[4] P. Nandy, P. Bandyopadhyaya, A. Deya, R. Basu, and S. Das, "Synthesis and characterization of copper doped zinc oxide nanoparticles and its application in energy conversion," *Curr. Appl. Phys.*, vol. 14, pp. 1149-1155, 2014.

[5] E. Ozkaraoglu, I. Tunc, and S. Suzer, "Preparation of Au and Au-Pt nanoparticles within PMMA matrix using UV and X-ray irradiation," *Polymer*, vol. 50, pp. 462-466, 2009.

[6] B. Choudhary, S. Chawla, K. Jayanthi, K. N. Sood, and

[7] A. Singh, U. K. Kulkarni, and C. Khan-Malek, "Patterning of SiO_2 nanoparticle-PMMA polymer composite microstructures based on soft lithographic techniques," *Microelectron. Eng.*, vol. 88, pp. 939-944, 2011.

[8] A. Silva, K. Dahmouche, and B. Soares, "The effect *of* addition *of* acrylic acid and thioglycolic acid on the nanostructure and thermal stability of PMMA montmorillonite nanocomposites," *Appl. Clay Sci.*, vol. 47, pp. 414-420, 2010.

[9] W. Ma, J. Zhang, X. Wang, and S. Wang, "Effect of PMMA on crystallization behavior and hydrophilicity of poly(vinylidene fluoride)/poly(methyl methacrylate) blend prepared in semi-dilute solutions," *Appl. Surf. Sci.*, vol. 253, pp. 8377-8388, 2007.

[10] V. L. Schade, and T. S. Roukis, "The role of polymethyl methacrylate antibiotic-loaded cement in addition to debridement for the treatment of soft tissue and osseous infections of the foot and ankle," *J. Foot Ankle Surg.*, vol. 49, pp. 55-62, 2010.

[11] S. P. Mohanty, M. N. Kumar, and N. S. Murthy, "Use of antibiotic-loaded polymethyl methacrylate beads in the management of musculoskeletal sepsis - a retrospective study," *J. Orthop. Surg.*, vol. 11, pp. 73-79, 2003.

[12] N. L. Pleshko, A. L. Boskey, and R. Mendelsohn, "An infrared study of the interaction of polymethyl methacrylate with the protein and mineral components of bone," *J. Histochem. Cytochem.*, vol. 40, pp. 1413-1417, 1992.

[13] A. Stevens, and J. Germain, *The Theory and Practice of Histological Techniques*, 3rd Ed., Resin Embedding Media, J. D. Bancroft, and A. Stevens, Eds. New York, Churchill Livingstone, 1990.

[14] S. A. Elawam, W. M. Morsi, H. M. Abou-Shady, and W. G. Osiris, "Characterizations of beta-lead oxide "massicot" nano-particles," *Brit. J. Appl. Sci. Technol.*, vol. 17, pp. 1-10, 2016.

[15] S. Li, W. Yang, M. Chen, J. Gao, J. Kang, and Y. Qi, "Preparation of PbO nanoparticles by microwave irradiation and their application to Pb(II)-selective electrode based on cellulose acetate," *Mater. Chem. Phys.*, vol. 90, pp. 262-269, 2005.

[16] B. Jia, and L. Gao, "Synthesis and characterization of single crystalline PbO nanorods via a facile hydro-thermal method," *Mater. Chem. Phys.*, vol. 100, pp. 351-354, 2006.

[17] M. M. Kashani-Motlagh, and M. K. Mahmoudabad, "Synthesis and characterization of lead oxide nano-powders by sol-gel method," *J. Sol-Gel Sci. Techn.*, vol. 59, pp. 106-110, 2011.

[18] L. Li, X. Zhu, D. Yang, L. Gao, J. Liu, R. V. Kumar, and J. Yang, "Preparation and characterization of nano-structured lead oxide from spent lead acid battery paste," *J. Hazard. Mater.*, vol. 203, pp. 274-282, 2012.

[19] A. El-Sayed Abdo, M. A. M. Ali, and M. R. Ismail, "Natural fibre high-density polyethylene and lead oxide composites for radiation shielding," *Phys. Chem.*, vol. 66, pp. 185-195, 2003.

[20] W. H. Zhong, G. Sui, S. Jana, and J. Miller, "Cosmic radiation shielding tests for UHMWPE fiber/nano-epoxy composites," *Compos. Sci. Technol.*, vol. 69, pp. 2093-2097, 2009.

[21] M. Erdem, O. Baykara, M. Dogru, and F. Kuluozturk, "A novel shielding material prepared from solid waste containing lead for gamma ray," *Radiat. Phys. Chem.*, vol. 79, pp. 917-922, 2010.

[22] V. Harish, N. Nagauah, T. N. Prabhu, and K. T. Varughese, "Thermo-mechanical analysis of lead monoxide filled unsaturated polyester based polymer composite radiation shields," *J. Appl. Polym. Sci.*, vol. 117, pp. 3623-3629, 2010.

[23] Y. R. Uhm, J. Kim, S. Lee, J. Jeon, and C. K. Rhee, "In situ fabrication of surface modified lead monoxide nanopowder and its HDPE nanocomposite," *Ind. Eng. Chem. Res.*, vol. 50, pp. 4478-4483, 2011.

S. Singh, "The effect of Al and B on the luminescent property of porous silicon," *Curr. Appl. Phys.*, vol. 10, pp. 807-812, 2010.

[24] K. E. Geckeler, and H. Nishide, *Advanced Nanomaterial*, Wiley-VCH Verlag GmbH & Co. KGaA, Weinheim, 2011.

[25] A. Hassen, A. M. El Sayed, W. M. Morsi, and S. El-Sayed, "Influence of Cr_2O_3 nanoparticles on the physical properties of polyvinyl alcohol," *J. Appl. Phys.*, vol. 112, pp. 093525, 2012.

[26] A. M. El Sayed, and W. M. Morsi, "Dielectric relaxation and optical properties of polyvinyl chloride/lead monoxide nanocomposites," *Polym. Composite.*, vol. 34, pp. 2031-2039, 2013.

[27] A. M. El Sayed, and W. M. Morsi, "α-Fe_2O_3/(PVA + PEG) nanocomposite films; synthesis, optical, and dielectric characterizations," *J. Mater. Sci.*, vol. 49, pp. 5378-5387, 2014.

[28] A. M. El Sayed, S. El-Gamal, W. M. Morsi, and Gh. Mohammed, "Effect of PVA and copper oxide nanoparticles on the structural, optical, and electrical properties of carboxymethyl cellulose films," *J. Mater. Sci.*, vol. 50, 4717-4728, 2015.

[29] P. D. Anderson, M. Prusty, B. J. Keestra, and J. G. P. Goossens, "Experimental and computational study on structure development of PMMA/SAN blends," *Chem. Eng. Sci.*, vol. 62, 1825-1837, 2007.

[30] Ismayil, V. Ravindrachary, R. F. Bhajantri, S. D. Praveena, Boja Poojary, Dhanadeep Dutta, and P. K. Pujari, "Optical and microstructural studies on electron irradiated PMMA: A positron annihilation study," *Polym. Degrad. Stabil.*, vol. 95, 1083-1091, 2010.

[31] M. S. Khan, R. A. Qazi, and M. S. Wahid, "Miscibility studies of PVC/PMMA and PS/PMMA blends by dilute solution viscometry and FTIR," *Afr. J. Pure Appl. Chem.*, vol. 2, pp. 41-45, 2008.

[32] L. Peng, Y. Luo, Y. Dan, L. Zhang, Q. Zhang, S. Xia, and X. Zhang, "The study of preparation and luminescence of poly(methyl methacrylate)/rare earth composite luminescent materials," *Colloid Polym. Sci.*, vol. 285, pp. 153-160, 2006.

[33] A. Sarı, C. Alkan, and A. Karaipekli, "Preparation, characterization and thermal properties of PMMA/n-heptadecane microcapsules as novel solid–liquid micro PCM for thermal energy storage," *Appl. Energ.*, vol. 87, pp. 1529-1534, 2010.

[34] O. H. Kim, K. Lee, K. Kim, B. H. Lee, and S. Choe, "Effect of PVA in dispersion polymerization of MMA," *Polymer*, vol. 47, pp. 1953-1959, 2006.

[35] N. A. El- Zaher, M. S. Melegy, and W. G. Osiris, "Thermal and structural analyses of PMMA/TiO_2 nanoparticles composites," *Nat. Sci.*, vol. 6, pp. 859-870, 2014.

[36] E. M. Abdelrazek, I. S. Elashmawi, A. El-Khodary, and A. Yassin, "Structural, optical, thermal and electrical studies on PVA/PVP blends filled with lithium bromide," *Curr. Appl. Phys.*, vol. 10, pp. 607-613, 2010.

[37] K. Pielichowski, and J. Njuguna, *Thermal Degradation of Polymeric Materials*, Smithers Rapra Technlogy, 2005.

[38] M. C. Costache, M. J. Heidecker, E. Manias, and C. A. Wilkie, "The thermal degradation of PMMA nanocomposites with montmorillonite, layered double hydroxides and carbon nanotubes," *Polym. Advn. Technol.*, vol. 17, pp. 272-280, 2006.

[39] B. J. Holland, and J. N. Hay, "The kinetics and mechanisms of the thermal degradation of poly(methyl methacrylate) studied by thermal analysis-Fourier transform infrared spectroscopy," *Polymer*, vol. 42, pp. 4825-4835, 2001.

[40] J. H. Kim, J. Y. Kim, Y. M. Lee, and K. Y. Kim, "Properties and swelling characteristics of crosslinked poly(vinyl alcohol)/chitosan blend membrane," J. Appl. *Polym. Sci.*, vol. 45, pp. 1711-1717, 1992.